Bioorganic Chemistry 100 (2020) 103885

Contents lists available at ScienceDirect

Bioorganic Chemistry

journal homepage: www.elsevier.com/locate/bioorg

# Antibacterial activities and DNA-cleavage properties of novel fluorescent imidazo-phenanthroline derivatives

Aslıhan Yılmaz Obalı[a,*], Sedef Akçaalan[b], Emine Arslan[c], İhsan Obalı[c]

[a] Department of Chemistry, Faculty of Science, Selcuk University, Turkey
[b] Department of Molecular Biology and Genetics, Faculty of Science, Necmettin Erbakan University, Turkey
[c] Department of Biology, Faculty of Science, Selcuk University, Turkey

ARTICLE INFO

*Keywords:*
Imidazo-phenanthroline
Schiff base
Chloro-quinoline
Antimicrobial activity
DNA cleavage activity

ABSTRACT

Design and biological activities of fluorescent imidazo-phenanthroline derivatives; (*E*)-5-((4-((4-(1*H*-imidazo[4,5-*f*][1,10]phenanthrolin-2-yl)phenoxy)methyl)benzylidene)amino)-isophthalicacid, **2** and 2-(4-(((5-chloroquinolin-8-yl)oxy)methyl)phenyl)-1*H*-imidazo[4,5*f*] [1,10]phenanthroline, **3,** have been reported. Their characterizations were performed by spectroscopic techniques. Their promising photophysical behaviours were observed in absorbance and fluorescence studies. The antibacterial activities of the compounds were determined against seven different microorganisms; *Bacillus subtilis* ATCC 6633(G + ), *Pseudomonas aeruginosa* ATCC 29853(G-), *Escherichia coli* ATCC 35,218 (G-), *Enterococcus faecalis* ATCC 292,112 (G + ), *Salmonella typhimurium* ST-10 (G-), *Streptococcus mutans* NCTC 10,449 (G + ), and *Staphylococcus aureus* ATCC 25923(G + ). MIC values of **3** was determined as 156,25 μM on all tested bacteria. A preliminary study of the structure–activity relationship (SAR) also revealed that the antimicrobial activity depended on the substituents on the phenyl ring. The electron withdrawing Cl-substitued compound **3** most favour for antimicrobial activity even at lowest concentration compared to other compounds. DNA-cleavage activities of the compounds were also investigated. The interactions of the compounds with supercoiled pBR322 plasmid DNA were obtained by agarose gel electrophoresis. All imidazo-phenanthroline derivatives were found to be highly effective on DNA, even at the lowest concentrations because of their planar nature which provides ease of bind to the helix structure of DNA.

## 1. Introduction

Heterocyclic organic molecules such as imidazoles, imidazo-phenanthrolines, phenanthro-imidazoles and their derivatives bearing polar heteroatoms such as N, O in their aromatic π-conjugated rings were preferable in photophysical and biological studies [1–5]. Imidazo-phenanthrolines act as an electron acceptor in systems with their electron density deficiency on ***C*** atoms in aromatic ring. Donating/withdrawing substitutions to the imidazole-phenanthrolines increase the hyperpolarizability and effects their photophysical properties with the increase of intensity or shift of bands [6–9]. Hence, beside their considerable photophysical, pharmacological properties, imidazo-phenanthrolines exhibit also biological activity and DNA binding/cleavage properties, as well. To compare with other heterocylic molecules, imidazo-phenanthrolines have structural similarity with the amino acid histidine, vitamin B12, DNA base in living systems [10,11]. Furthermore, their planar nature provides ease of binding to the helix structure of DNA [12,13]. These features tend to increase the attention and use of imidazo-phenanthrolines in extensive sensor designs for ions or DNA and as agents for anticancer, antibacterial, antifungal, antitumour and antiflammatory drugs [14,15]. To increase the effect of biological activities or photophysical properties, derivation of those imidazole compounds with Schiff base or chloro-quinoline groups becomes an important issue.

Schiff bases with azomethine linkages which also exist in living systems can be used to understand the relationships between biomolecules and drug molecules and are very vital for improving the bioactive drugs. The effects of the quinolines in biological studies can be explained by the fact that they can penetrate bacterial cells and to inhibit DNA gyrase [16–32]. In this work, the design and synthesis of the Schiff base and quinoline based heterocylic imidazo-phenanthroline derivatives were designed for biological activity and photophysical studies. **2** was obtained by Schiff base condensation reaction and **3** was obtained by nucleophilic substitution of bromine-substitued imidazo-

* Corresponding author.
*E-mail address:* aslihanyilmaz@selcuk.edu.tr (A.Y. Obalı).

https://doi.org/10.1016/j.bioorg.2020.103885
Received 15 February 2020; Received in revised form 23 March 2020; Accepted 23 April 2020
Available online 03 May 2020

phenanthroline and 5-chloro-8-quinolinol. Their structures were well characterized.

## 2. Experimental section

### 2.1. Materials and instrumentation

The reagents and chemicals were purchased from Merck and Sigma-Aldrich and used without further purification. Melting points were determined by Büchi Melting Point B-540 instrument. $^1$H NMR and $^{13}$C NMR spectra were recorded on a Varian 400-MHz Spectrometer and Bruker Biospin 300-MHz Spectrometer, respectively. Infrared spectra were measured using a Bruker Fourier Transform-Infrared (FT-IR) Spectrometer. Elemental analyses were carried out using a LECO-CHNS-932 elemental analyzer. High-Resolution Mass Spectroscopy was recorded on Waters SYNAPT G1 MS at positive mode (ES + )50–1000 Da. UV–vis spectra were recorded on Perkin Elmer Lambda 25 UV–Vis Spectrometer. Fluorescence data were obtained by using a Perkin Elmer LS 55 Luminescence Spectrometer. All measurements were carried out at 298 K. Thin layer chromatography (TLC) plates were supplied from merck (silica gel 60 F254 on aluminum.

### 2.2. Synthesis procedures

1,10-Phenantroline-5,6-dione, 4-(1*H*-imidazo[4,5–f][1,10]phenanthroline-2-yl)phenol **(1)**, 2-(4-(bromomethyl)phenyl)-1*H*-imidazo[4,5-f][1,10]phenanthroline, 4-((4-(1*H*-imidazo-[4, 5-*f*][1,10]phenanthrolin-2-yl)-phenoxy)methyl)benzaldehyde were synthesized *via* the literature methods [33,34].

***1,10-Phenantroline-5,6-dione.*** *1,10-Phenanthroline* (0.54 g, 3 mmol) was added into a solution of 60% sulfuric acid (7 mL). After the solid compound was dissolved, *potassium bromate* (0.55 g, 3.3 mmol) was added in batches over a period of half an hour. The mixture was stirred at room temperature for 20 h. Then, the mixture was poured over ice and was carefully neutralized to pH:7 using a saturated solution of sodium hydroxide. The solution was then filtered, extracted with dichloromethane and evaporated to dryness. The crude product was recrystallized from methanol to provide the desired product.

***4-(1H-imidazo[4,5-f]***[1,10]***phenanthroline-2-yl)phenol, 1.*** *1,10-Phenanthroline-5,6-dione* (0.1 g, 0.46 mmol) and ammonium acetate (0.58 g, 13.3 mmol) were dissolved in 10 mL of hot glacial acetic acid. While the mixture was stirred, a solution of *4-hydroxybenzaldehyde* (0.056 g, 0.46 mmol) in 10 mL of glacial acetic acid was added dropwise to the mixture. The mixture was heated at 90 °C for 3 h and was then poured in 200 mL of water. The solution was neutralized with ammonia to pH:7 and was then cooled to room temperature. The precipitate was filtered off and washed with large portions of water. The product was dried for 48 h in a vacuum at 50 °C.

***2-(4-(bromomethyl)phenyl)-1H-imidazo[4,5-f]***[1,10]***phenanthroline.*** A mixture of *1,10-phenanthroline-5,6-dione* (0.25 g, 1.2 mmol), ammonium acetate (2.6 g, 1.2 mmol), *4-(bromomethyl)benzaldehyde* (0.25 g, 0.46 mmol) and 30 mL glacial acetic acid were refluxed for 48 h and then poured in 200 mL of water. The solution was neutralized with ammonia to pH:7 and cooled to room temperature. The precipitate was collected and washed with water. The crude yellow product was dried under vacuum.

***4-((4-(1H-imidazo[4,5-f]***[1,10]***phenanthrolin-2-yl)-phenoxy)methyl)benzaldehyde.*** To the solution of *4-(bromomethyl)benzaldehyde* in 30 mL DMF, *4-(1H-imidazo[4,5-f]*[1,10] *phenanthroline-2-yl)phenol* (0.15 g, 0.5 mmol) and $K_2CO_3$ (0.13 g, 1 mmol) were added. The mixture was stirred for 36 h at 90 °C. Then cooled to room temperature and 50 mL water as added to the solution. The resulting crude product were filtered and washed with cold water.

***(E)-5-((4-((4-(1H-imidazo[4,5-f]***[1,10]***phenanthrolin-2-yl)phenoxy)methyl)benzylidene) amino)isophthalic acid, 2.*** Schiff base condensation reaction of *5-aminoisophthalic acid* (0.04 g, 0.23 mmol) and *4-((4-(1H-imidazo[4,5-f]*[1,10]*phenanthrolin-2-yl)phenoxy)methyl)-benzaldehyde* (0.1 g, 0.23 mmol) were carried out in 30 mL methanol medium under reflux for 72 h. The reaction was monitored by TLC by using methanol/$NH_3$ (4: 1) as the eluent. The crude dark yellow residue was collected by filtration and washed with methanol and dried under vacuum (yield %86). M.P. > 300 °C (decomp.). FT-IR υ($cm^{-1}$): 3393 (OH), 3055 (NH), 2870 (CH), 1683 (C═N), 1611 (C═O), 1248 (C−O−C). $^1$H NMR (DMSO-$d_6$) δ(ppm): 13.80 (b, s, 1H, N***H***), 13.12 (b, s, 2H, O***H***), 8.92 (s, 1H, ***H***C = N), 9.1–7.3 (m, 17H, aromatic-C***H***), 5.45 (s, 2H, O-C***H₂***). $^{13}$C NMR (DMSO-$d_6$): $\delta$ (ppm) = 168, 167, 161, 160, 153, 152, 151, 149, 148, 145, 136, 134, 133, 131, 130, 129, 127, 124, 119, 118, 116, 69. Elemental analysis ($C_{35}H_{23}N_5O_5$), Calculated (Found) %: C: 70.82 (70.74), H: 3.91 (3.89), N: 11.80 (11.73).

***2-(4-(((5-chloroquinolin-8-yl)oxy)methyl)phenyl)-1H-imidazo[4,5-f]***[1,10]***phenanthroline, 3.*** *5-Chloro-8-quinolinol* (0.046 g, 0.25 mmol) was dissolved in 30 mL methanol and then added dropwise to the methanol solution of *2-(4-(bromomethyl)phenyl)-1H-imidazo[4,5-f]*[1,10]-*phenanthroline* (0.1 g, 0.25 mmol) and triethylamine (0.034 mL, 0.25 mmol). The mixture was refluxed for 48 h. The reaction was monitored by TLC by using methanol/$NH_3$ (4: 1) as the eluent. After the reaction completed, evaporation of the solvents were performed. Light yellow solid residue was washed with water. Then dried under vacuum. (yield %90). M.P. > 300 °C (decomp.). FT-IR υ($cm^{-1}$): 3151 (NH), 2921 (CH), 1651 (C═N), 1279 (C−O−C), 550 (C-Cl). $^1$H NMR (DMSO-$d_6$) δ(ppm): 13.66 (b, s, 1H, N***H***), 9.2–7.3 (m, 15H, aromatic-C***H***), 4.85 (s, 2H, O-C***H₂***). $^{13}$C NMR (DMSO-$d_6$): $\delta$ (ppm) = 157, 153, 152, 150, 148, 145, 142, 135, 134, 133, 129, 128, 127, 124, 123, 118, 116, 115, 107, 71. Elemental analysis ($C_{29}H_{18}ClN_5O$), Calculated (Found) %: C: 71.38 (71.34), H: 3.72 (3.64), N: 14.35 (14.28). HRMS (ESI) (*m/z*) $(M + H)^+$: 488.12.

### 2.3. Antimicrobial activities

In antimicrobial activity studies, the minimum inhibitory concentration values of compounds were determined by using broth microdilution method. Antibacterial activity of compound individually tested against different microorganisms *[Bacillus subtilis* ATCC 6633(G + ), *Pseudomonas aeruginosa* ATCC 29853(G-), *Escherichia coli* ATCC 35,218 (G-), *Enterococcus faecalis* ATCC 292,112 (G + ), *Salmonella typhimurium* ST-10 (G-), *Streptococcus mutans* NCTC 10,449 (G + ), and *Staphylococcus aureus* ATCC 25923(G + )]. Gram positive and gram negative bacteria were grown on Mueller-Hinton agar plates and incubated at 37 °C for 24 h.

MIC value was determined by using microplate. The bacterial suspensions were adjusted to 0.5 McFarland standard turbidity ($10^8$ CFU/ml). Finally, these suspensions used as inoculums were prepared at $10^5$ CFU/ml by diluting fresh cultures at McFarland 0.5 density. Mueller-Hinton Broth (100 µl) was placed into each 96 wells of microplates. Compound solutions initially prepared at a concentration of 10000 µM were added into first wells of microplates and two fold dilutions of the compounds (2500–2,44 µM) were made by dispensing the solutions to the remaining wells. Then, 100 µl of culture suspensions were inoculated to each well. Chloramphenicol (2500–2,44 µM) was used as control. The sealed microplates were incubated at 37 °C for 24 h. Microbial growth was determined by adding 200 µl of 2,3,5-Triphenyltetrazolium chloride (0.5%) after incubation to each well and incubating for 30 min at 37 °C. The lowest concentration of the compounds that completely inhibit macroscopic growth was determined as minimum inhibitory concentrations (MICs).

### 2.4. DNA cleavage activity

The interactions of the compounds with supercoiled pBR322 plasmid DNA were studied by agarose gel electrophoresis. The complexes were incubated with pBR322 DNA in the dark at 37 °C for 24 h and electrophoresed in 1% agarose gel electrophoresis. The gel was

electrophoresed for 1 h at 100 V in 1XTAE buffer. After electrophoresis, the gel was stained in ethidium bromide, then, DNA viewed with UV-transilluminator.

### 2.5. BamH I and Hind III restriction enzyme digestion

The compound-DNA mixtures were first incubated for 24 h and then restricted with restriction enzyme *BamH* I and *Hind* III for 1 h at 37 °C. *BamH* I and *Hind* III are known to recognize the sequence G/GATCC and A/AGCTT respectively. pBR322 plasmid DNA contains a single restriction site for each enzyme which convert supercoiled form I DNA and singly nicked circular Form II DNA to linear form III DNA. After one hour incubation, the restricted DNA was electrophoresed in 1% agarose gel for 1 h at 100 V in TAE buffer. The gel was stained with ethidium bromide and then viewed with UV-transilluminator.

## 3. Results and discussion

### 3.1. Synthesis and characterizations

Herein we report the synthesis and characterization of imidazo-phenanthroline derivatives. 1,10-phenantroline-5,6-dione and 4-(1*H*-imidazo[4,5-f][1,10]phenanthroline-2-yl)phenol, **1** were synthesized *via* the literature method (and also given in experimental part) and obtained for the next steps. **2** was obtained by the Schiff base condensation reaction between 4-((4-(1*H*-imidazo[4,5-*f*][1,10]-phenanthrolin-2-yl)-phenoxy)methyl)benzaldehyde and 5-aminoisophthalic acid. It precipitated in 1 h with good yields. Because of the difficulties in purifying Schiff bases in column chromatography, **2** was purified by washing with methanol several times. The reactions of the starting compounds and target compounds are demonstrated in Scheme 1. The reaction of 5-chloro-8-quinolinol and 2-(4-(bromomethyl)-phenyl)-1H-imidazo[4,5-f][1,10]-phenanthroline in the presence of triethylamine gave chloro-quinoline based imidazo-phenanthroline derivative, **3** (Scheme 2).

The structures of the compounds were confirmed by melting point measurements and FT-IR, $^{1}$H NMR, $^{13}$C NMR, HRMS techniques. Melting points of the compounds were determined at room temperature. The melting point differences between the starting compounds and target compounds primarily can prove the synthesis of target compounds. FT-IR spectra of the compounds are given in Figs. 1–2. For the Schiff base compound **2**, the bands appeared at 3462 cm$^{-1}$, 3056 cm$^{-1}$, 1683 cm$^{-1}$ can be attributed to υ(OH, carboxylic acid), υ(NH) and υ(C=N), respectively. The azomethine band is the most specific band for **2**. For the chloro-quinoline based compound **3**, the bands at 3151 cm$^{-1}$, 1651 cm$^{-1}$, 1279 cm$^{-1}$, 551 cm$^{-1}$ can be assigned to υ(NH), υ(C=N), υ(C−O−C), υ(C-Cl), respectively. The disappears of υ(OH) band of 5-chloro-8-quinoline and formation of υ(C−O−C) etheric band proves the synthesis of target compound **3**. $^{1}$H NMR spectra of the compounds are given in experimental part (Figs. 3 and 5). The broad singlet peak at 13.12 ppm is assigned for the carboxylic acid OH protons of **2**. Another important singlet that appears at 8.92 ppm is the proof of CH = N azomethine protons of the Schiff base **2**. For **3**, the most specific peak appears on $^{1}$H NMR spectra at 4.85 ppm is of O-CH$_2$ protons. Absence of the aldehyde peak and amine peak of the initial compounds proves the target compound **3**. Specific $^{13}$C NMR signals for **2** appeared at 69 ppm for oxy-bonded aliphatic carbon (O-CH$_2$), 152 ppm for the carbon which connects NH and N groups of imidazole unit, 160 ppm for imine carbon of Schiff base and 169 ppm for carboxylic acid carbons (Fig. 4). $^{13}$C NMR signals for **3** are appeared at 71 ppm for oxy-bonded aliphatic carbon (O-CH$_2$), 152 ppm for the carbon which connects NH and N groups of imidazole unit, 118 ppm for chloro-bonded aromatic quinoline carbon and 156 ppm for the oxy-bonded aromatic quinoline carbon (Fig. 6). HRMS (ESI) was also recorded for **3** to determine the molecular weight (Fig. 7). The molecular ion peak was observed at *m/z* 488.12 confirming the formula weight of **3** which is the same as the calculated value.

### 3.2. Photophysical properties

Absorption data of **1** (1x10$^{-5}$M), **2** (1x10$^{-5}$M) and **3** (1x10$^{-4}$M) were determined in acetonitrile. To explain the different concentration

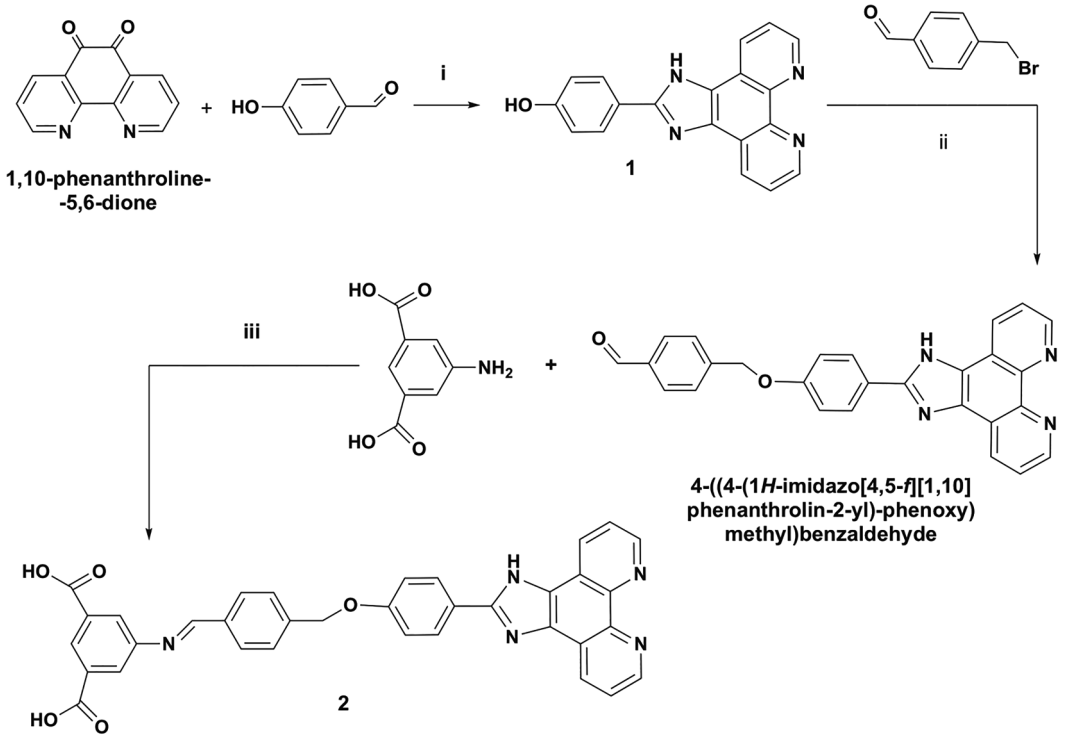


**Scheme 1.** Synthesis route of Schiff base imidazo-phenanthroline derivative, **2**. The reaction conditions were as **i)** ammonium acetate, glacial acetic acid, 118 °C. **ii)** $K_2CO_3$, DMF, 90 °C, **iii)** Methanol, 65 °C.

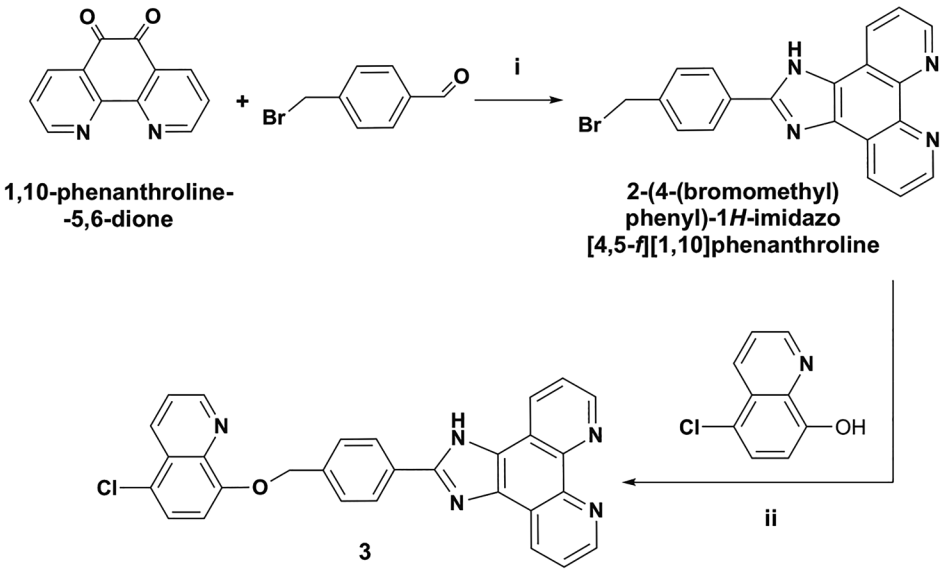


**Scheme 2.** Synthesis route of chloro-quinoline based imidazo-phenanthroline derivative, **3**. The reaction conditions were as **i)** ammonium acetate, glacial acetic acid, 118 ˚C, **ii)** triethylamine, methanol, 65 ˚C.

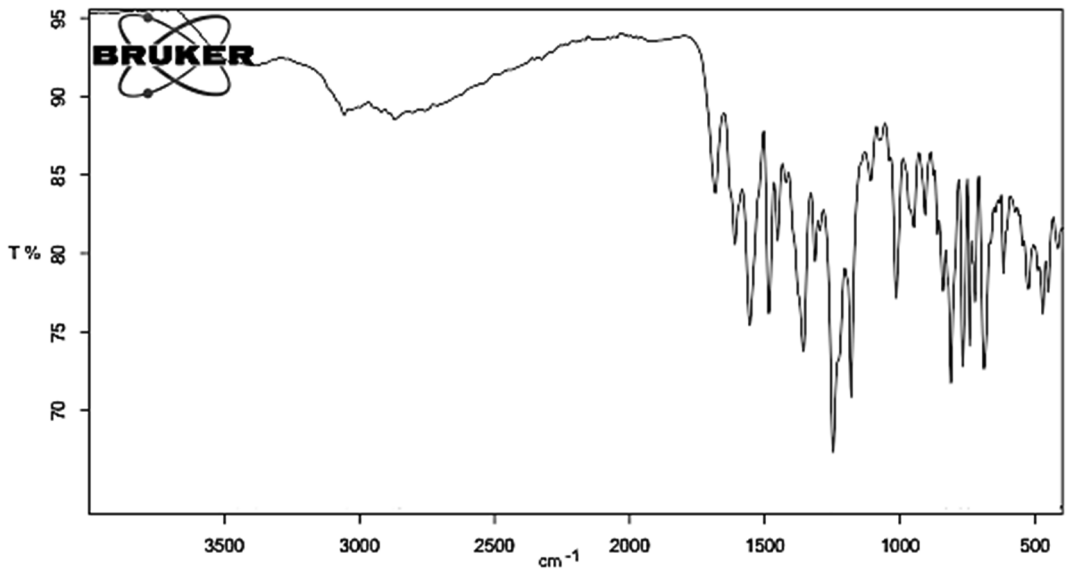


**Fig. 1.** FT-IR spectrum of (*E*)-5-((4-((4-(1*H*-imidazo[4,5–f][1,10]phenanthrolin-2-yl)phenoxy)methyl)benzylidene)-amino)isophthalic acid, **2**.

preference of **3**, it should be noted that at lower concentrations (such as $1x10^{-5}$M) very low absorbance data were recorded. Hence, higher concentration ($1x10^{-4}$M) was preferred to see the double shoulders clearly for **3**. All the compounds show absorbances in UV–vis region. The spectra of **1, 2** and **3** exhibit double shoulder bands at λ: 280–324 nm, 280–324 nm and 280–314 nm, respectively (Fig. 8). These bands correspond to phenanthroline-centered spin-allowed π → π* transitions [35]. Molar absorptivities, ε, were calculated as 120.000 $M^{-1}.cm^{-1}$, 80.000 $M^{-1}.cm^{-1}$ and 18.000 $M^{-1}.cm^{-1}$ for the compounds **1**, **2**, and **3** (respectively) at their maximum absorbances and $\lambda_{max}$: 280 nm for each**.**

Fluorescence studies of **1**, **2** and **3** in acetonitrile medium (both $1x10^{-4}$M and $1x10^{-5}$M) were also reported at the excitation of λ: 270 nm. When excitated at 270 nm, exhibited fluorescence bands for all the compounds are displayed in Fig. 9**.** The effects of concentration increases on fluorescence intensities were also observed. The solutions of three compounds were prepared with concentrations of $1x10^{-4}$M and $1x10^{-5}$M. Red-shifts from λ: 329–370 nm to 372–460 nm for **1**, from λ: 331–370 nm to 361–460 nm for **2** and from λ: 323–370 nm to 338–369 nm for **3** were observed. While recording the samples with more concentrated (as $1x10^{-2}$M) solutions, we observed the scala was passed over with noise so we couldn't record more concentrated solutions. Red-shifts might be occurred due to the intermolecular association of the molecule–molecule dimer aggregate formation in the ground state at high concentrations of solute. It was discovered that increasing the concentration of a dye molecule, band arises and red-shifted and aggregates formed. To form the simplest aggregate, a dimer, the dye–dye interaction must be strong enough to overcome any other forces which would favor solvation of the monomer [36,37]. And also the delocalization of electrons between π-conjugated the imidazo-phenanthroline rings may give rise to form a charge cloud above and below this plane along the conjugated chain and may cause red-shift in fluorescence band [38,39].

### *3.3. Antimicrobial activity*

The antibacterial activities of OH-substitued **(1)**, COOH-substitued **(2)** and Cl-substitued **(3)** imidazo-phenanthroline derivatives were

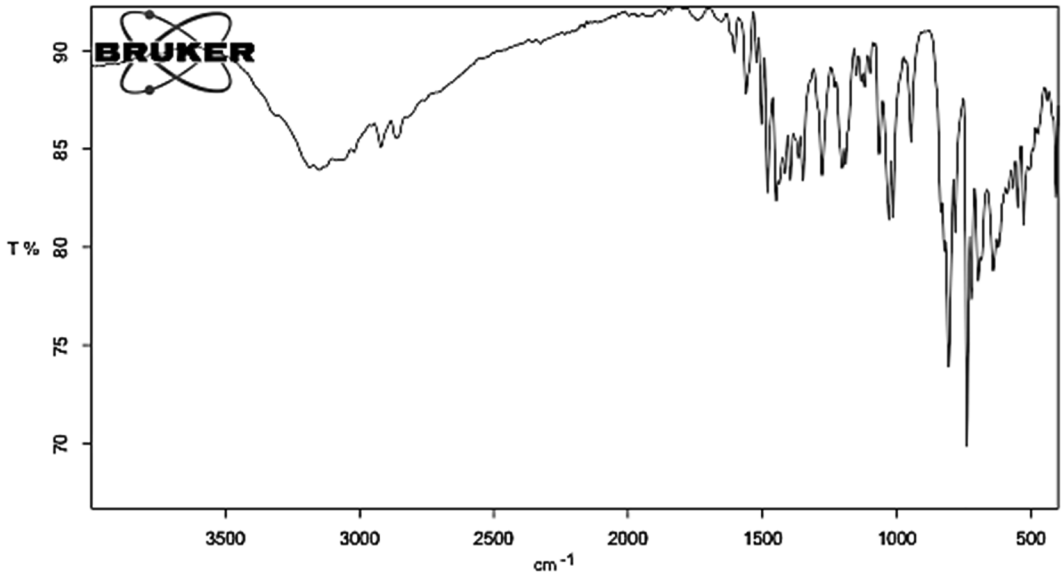


**Fig. 2.** FT-IR spectrum of 2-(4-(((5-chloroquinolin-8-yl)oxy)methyl)phenyl)-1*H*-imidazo[4,5*f*][1,10]phenanthroline, **3**.

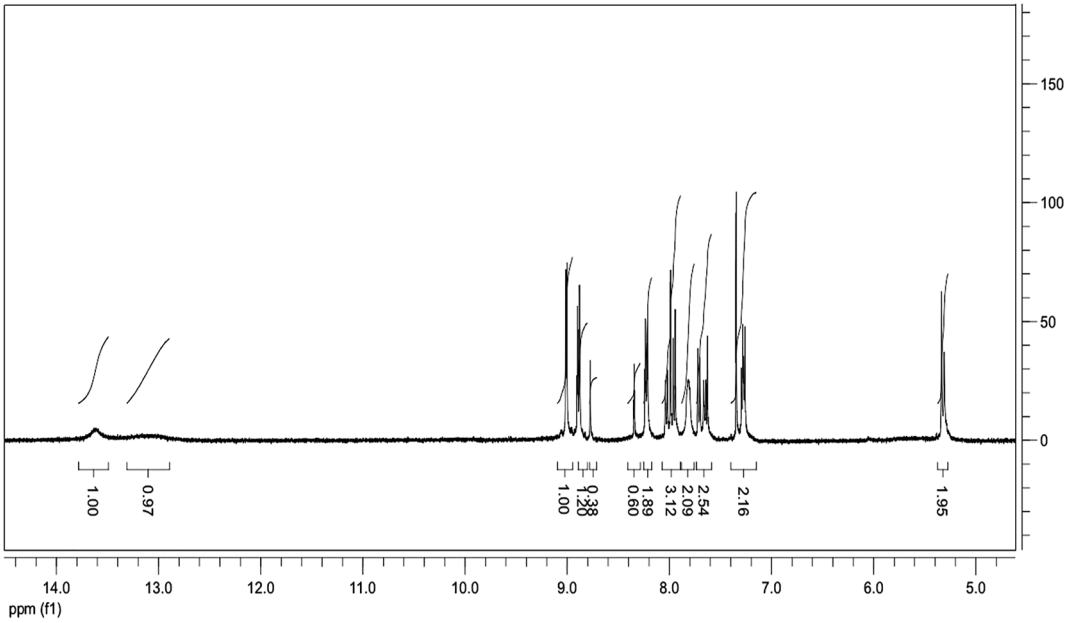


**Fig. 3.** $^{1}$H NMR spectra of Schiff base imidazo-phenanthroline derivative compound **2**.

determined against *B.subtilis, P.aeruginosa, E.coli, E.faecalis, S.typhimurium, S.mutans* and *S.aureus microorganisms*. The antimicrobial activities with minimum inhibitory concentrations (MIC) of the compounds are given in Table 1.

The minimal inhibitory concentration (MIC) values of the compounds were studied further, and these values are in the range of 156,25–1250 μM. Chloramphenicol was used as a control. As it is shown in Table 1, it can be seen that the most effective compound on the microorganisms was **3**. According to the results, the MIC values of **3** was determined as 156,25 μM on all tested bacteria. It is generally known that the existence of electron-donating groups on the phenyl ring such as OH reduce, electron-withdrawing groups such as Cl, COOH increase the antimicrobial activities. Hence, the results of this study were compatible with that knowledge that OH– substituted compound **1** has less antimicrobial activity at lower concentrations. Comparing the derivatives **1**, and **2**, even at lowest concentration **3** shows most antibacterial activity among them. According to the structure–activity relationships of OH–, COOH– and Cl- substitued imidazo-phenanthroline derivatives (Fig. 10) against microorganisms indicated that introduction of electron-withdrawing Cl boosted the antimicrobial activity and this leads compound **3** more potent than other compounds [40–41].

### 3.4. DNA cleavage activity; interaction with pBR322 plasmid DNA

At the highest two concentrations (10000 and 5000 μM) of **1**, both Form I and Form II bands disappear because of degradation of pBR322 plasmid DNA. In Fig. 11*(C)*, the mobility of Form I has increased and all of the concentrations of **1** were decreased intensity of Form I band compared with Form II but when further dilutions of this compound are made starting from the 7th concentration Fig. 12*(C)*, it has become closer to untreated plasmid in the decreasing concentrations of **1**. **1** clearly accelerated the migration of the open circular form (FormII) because of the condensation and cross-linking of DNA (shown in both

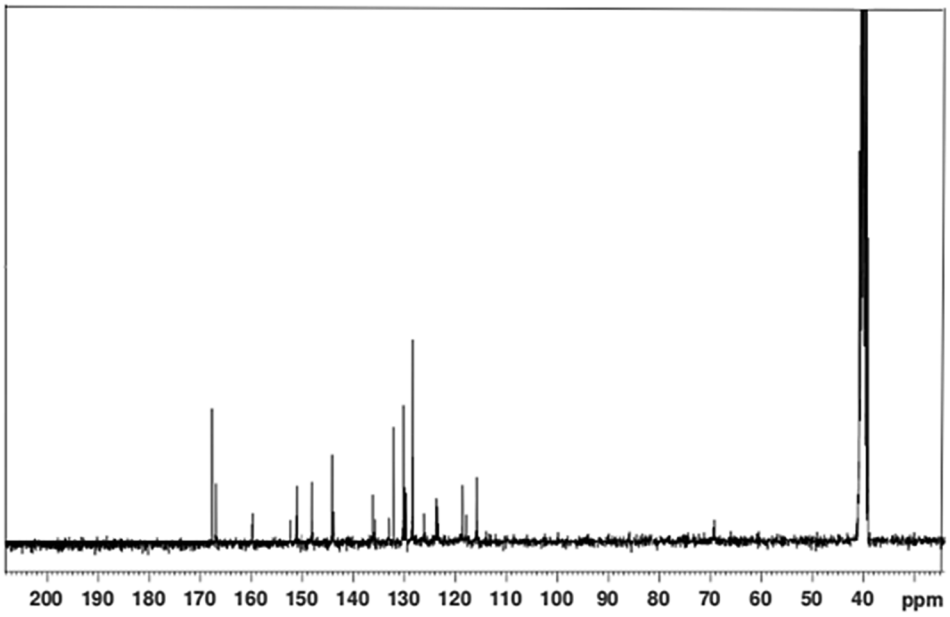


**Fig. 4.** $^{13}$C NMR spectra of Schiff base imidazo-phenanthroline derivative compound **2.**

Fig. 11*(C)* and Fig. 12*(C)*) [42–43].

In Fig. 11*(A)*, plasmid DNA bands are not visible at the first 6 concentrations at which the serial dilutions starting from 10000 μM are made. Therefore additional dilutions were made starting from the 7th concentration. As shown in Fig. 12*(A)*, the untreated plasmid was used a positive control and plasmid DNAs which incubated with **2** at concentrations between 156.25 and 1.220 μM were run. At the highest concentration (156.25) of **2**, both Form I and Form II bands disappear. This shows that **2** may be caused degradation of pBR322 plasmid DNA. All of the concentrations of **2** were decreased intensity of Form I band compared with Form II and **2** accelerated the migration of both the supercoiled form (Form I) and the open circular form (FormII). This is due to the condensation of DNA [42–43]. The intensity of the Form II band increased with decreasing concentrations.

Fig. 11*(B)* shows the electrophoretic mobility of the **3**-DNA mixture. In the highest first 7 concentrations of **3**-DNA interaction, the DNA has been completely degenerated. At the 8th and 9th concentrations, DNA may appear to be cleavaged while bands are invisible. Compared to other compounds, further dilutions were made an addition to concentrations which were less than these 7 concentrations and were found to be very effective even at the lowest concentrations (0.152 μM). The gel photo shows concentrations that decrease from 156.25 μM to 0.152 μM (Fig. 12*(B)*). Both Forms I and II were not detectable at the highest two concentrations of **3** (156.25 μM and 78.125 μM) when the plasmid DNA interacted with **3**. This shows that **3** may be caused degradation of pBR322 plasmid DNA. The electrophoretic mobility of both Form I and Form II was increased according to the control plasmid. All of the concentrations of **3** were decreased the intensity of Form I band.

All the three imidazo-phenanthroline derivative compounds studied

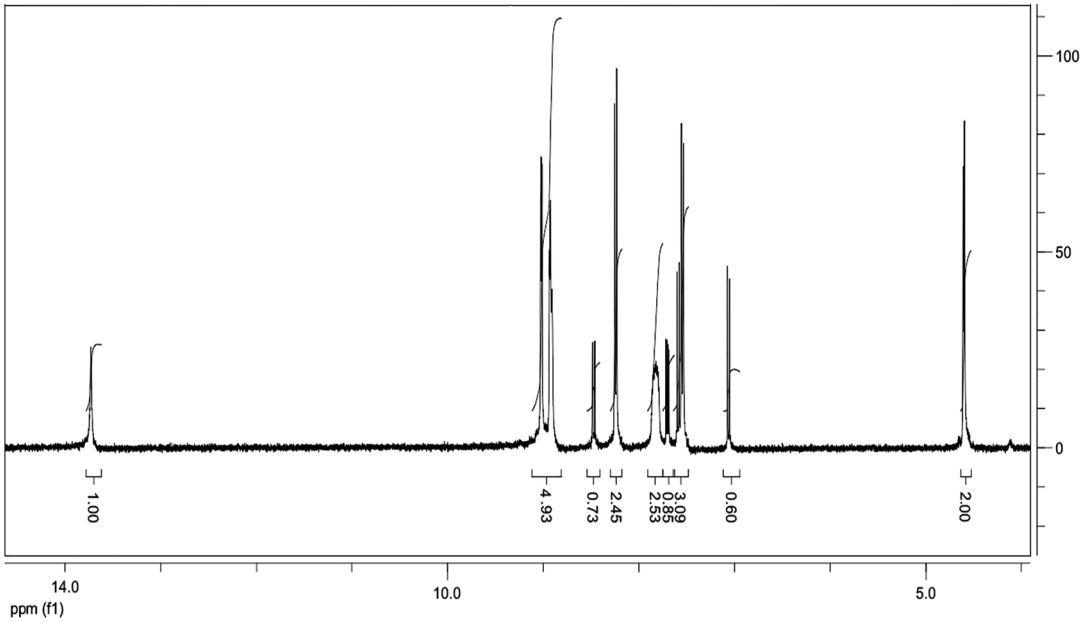


**Fig. 5.** $^{1}$H NMR spectra of chloro-quinoline based imidazo-phenanthroline derivative compound **3**.

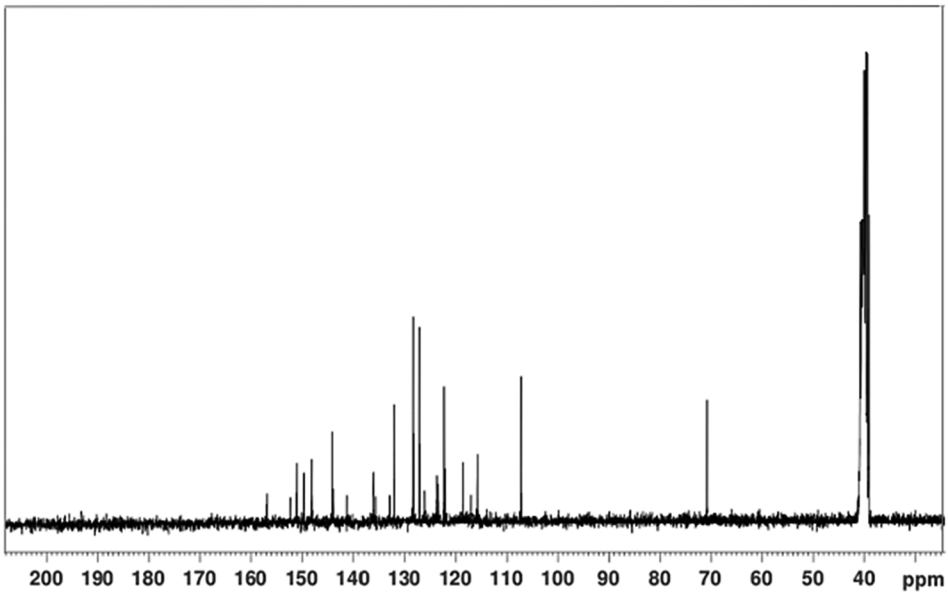


**Fig. 6.** $^{13}$C NMR spectra of chloro-quinoline based imidazo-phenanthroline derivative compound **3.**

were found to be highly effective on DNA, even at the lowest concentrations. But if we compare three of them, it was found to be the most effective **3,** since the DNA is degenerate as shown in Fig. 11*(B)*.

### *3.5. BamH I and Hind III restriction enzyme digestion of compound-plasmid DNA*

In order to assess whether the **1**, **2** and **3** show affinity toward guanine-guanine (GG) and/or adenine-adenine (AA) regions, the restriction endonuclease analysis of the compound-pBR322 plasmid DNA adducts was carried out by *BamH* I and *Hind* III enzymes and the electrophoretograms are shown in Fig. 13*(A), (B) and (C)*. *BamH* I and *Hind* III enzymes bind at the recognition site G-GATCC and A-AGCTT and cleave these sequences just after 5′-guanine and 5′-adenine sites, respectively, and, as a result, convert Form I and Form II DNA to linear Form III DNA. Therefore, the restriction enzymes have been used to observe that endonuclease activity is inhibited in the presence of complexes by binding or blocking the recognition sites in plasmid DNA [43–45].

The highest first 4 concentrations of **1**, All three forms of plasmid DNA forms were observed, though Form I and II were faint. **1** binds to G-G bases at these high doses and relatively inhibits the cleavage of Form I and II. However, at decreasing concentrations (last 4 concentrations), the compound was unable to inhibit to cut off with *Bam*HI both open circular and supercoil forms of plasmid DNA. The highest first 5 concentrations of **1**, all three forms of plasmid DNA forms were observed, though Form I and II were faint. But in the other decreasing concentrations, it was only observed Form III (Fig. 13*(C))*.

Digestion with *BamH* I and *Hind* III of **2**-DNA interaction disappear since at the highest first concentration of **2** was not detectable as to be **2**-DNA interaction test. Although the intensity of linear DNA (Form III) band increased in decreasing concentrations, intensity Form I and Form

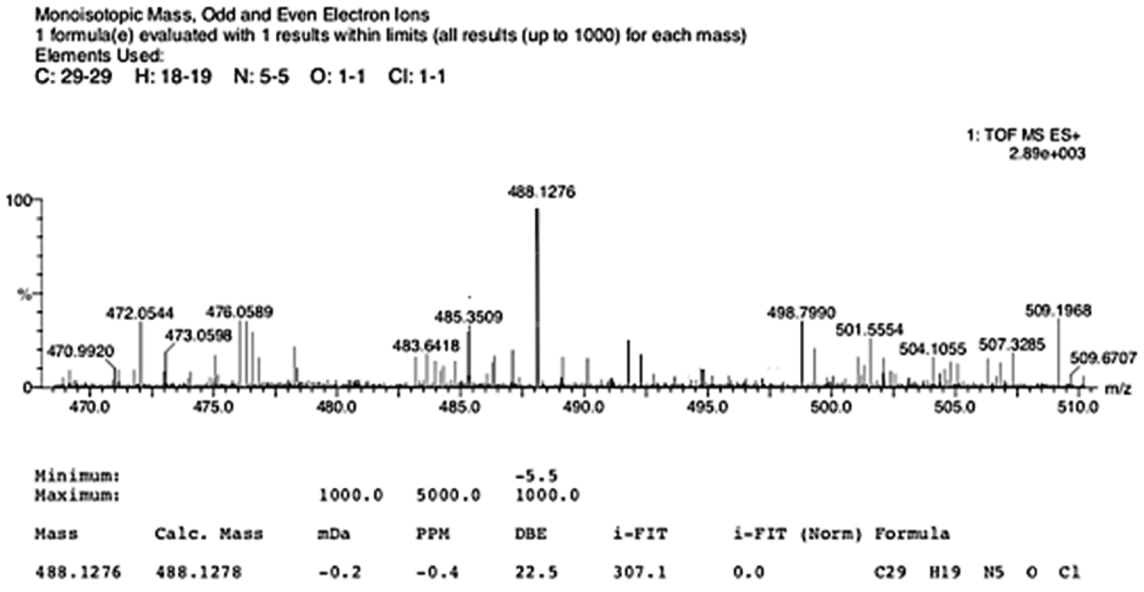


**Fig. 7.** HRMS spectra of chloro-quinoline based imidazo-phenanthroline derivative compound **3**.

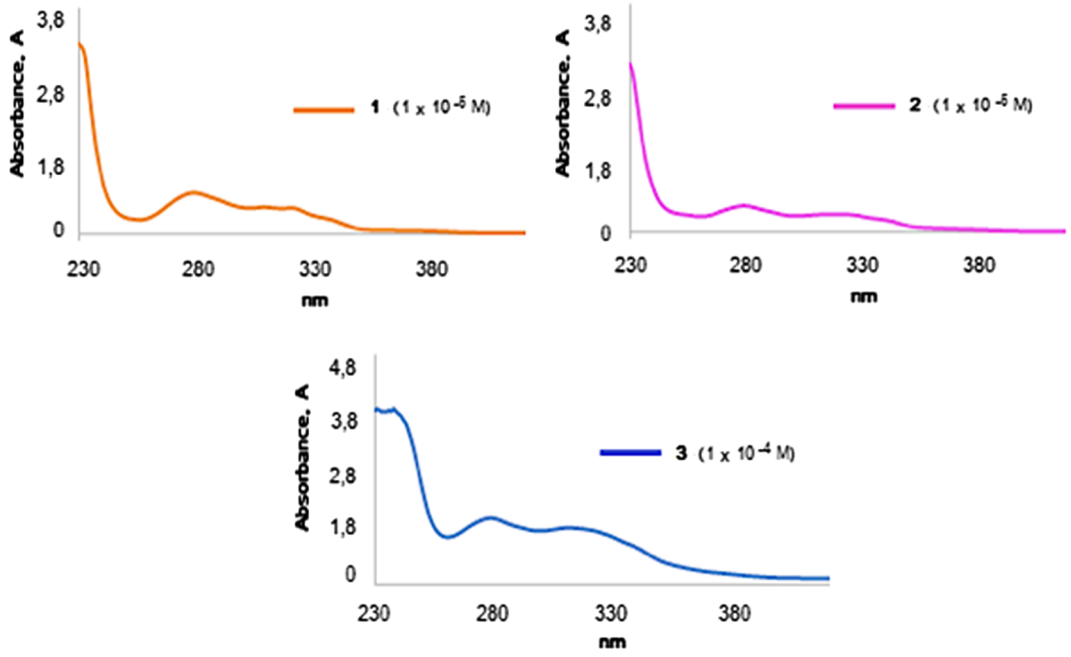


**Fig. 8.** The absorption spectra of 4-(1*H*-imidazo[4,5-f][1,10]phenanthroline-2-yl)phenol, **1**, (*E*)-5-((4-((4-(1*H*-imidazo[4,5-*f*][1,10]phenanthrolin-2-yl)phenoxy) methyl)benzylidene)-amino)isophthalic acid, **2** and 2-(4-(((5-chloroquinolin-8-yl)oxy)methyl)phenyl)-1*H*-imidazo[4,5*f*][1,10]phenanthroline, **3** in acetonitrile medium.

II bands decreased but not completely lost. This shows that the compound does not allow the *BamH* I enzyme to completely digest because it binds to G-G bases in DNA. *Hind* III completely cut off by targeting supercoil form (Form I) and convert it into Form III. At the highest 3rd, 4th, and 5th concentrations, it mostly digested Form II, but cut at all concentrations except these. This shows that **2** was unable to cleave because it binds to A-A bases in plasmid DNA, which is the open circular form (Form II) (Fig. 13*(A)*).

It wasn't observed any bands in the highest five concentrations of **3**. It was already quite effective compared to other compounds even at decreasing concentrations of **3**. Since the compound did not bind to open circular plasmid DNA, *BamH* I completely cut off Form II. After the 6th concentrate, the intensity of Form III increased at decreasing concentrations. Form I is seen at the lowest last 4 concentrations, though very faint. Here we can say that the compound binds to by targeting G-G bases in DNA in supercoil form (Form I) at low concentrations. The *Hind* III restriction enzyme completely cut off Form I and Form II at the last 4 concentrations and convert to Form III. This indicated that the compound did not bind to A-A bases (Fig. 13*(B)*).

In case decreasing concentrations of **1**, **2** and **3**, only linear Form III band was observed in the presence of *Hind* III indicating that all of the plasmid DNA is doubly nicked at A-A region. In case decreasing concentrations of only **1**, only linear Form III band was observed in the presence of *BamH* I indicating that all of the plasmid DNA is doubly nicked at G-G region.

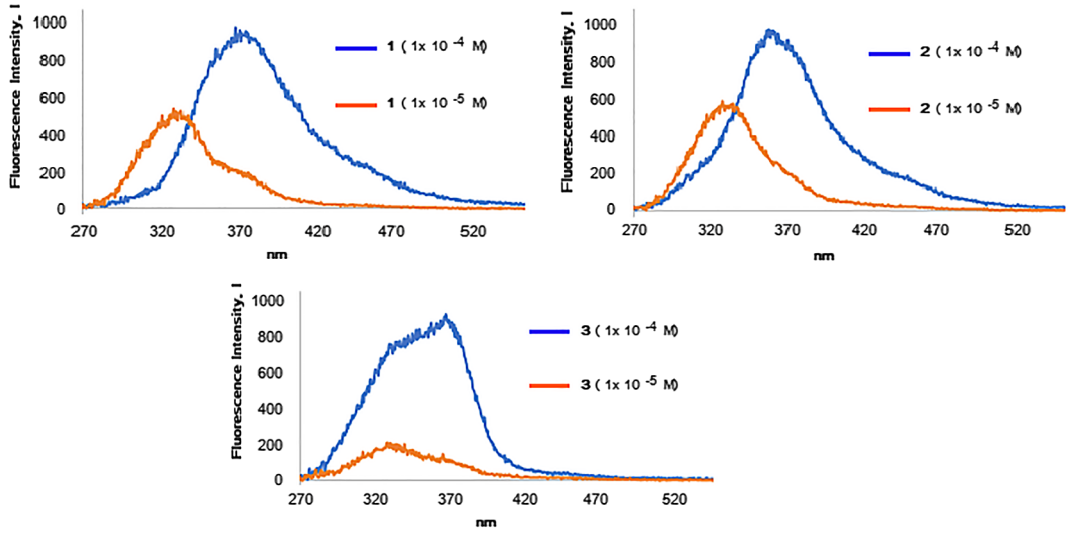


**Fig. 9.** The fluorescence spectra of 4-(1*H*-imidazo[4,5-f][1,10]phenanthroline-2-yl)phenol, **1**, (*E*)-5-((4-((4-(1*H*-imidazo[4,5-*f*][1,10]phenanthrolin-2-yl)phenoxy) methyl)benzylidene)-amino)isophthalic acid, **2** and 2-(4-(((5-chloroquinolin-8-yl)oxy)methyl)phenyl)-1*H*-imidazo[4,5*f*][1,10]phenanthroline, **3** with the concentrations of $1x10^{-4}$M and $1x10^{-5}$M in acetonitrile medium at $\lambda_{ext}$: 270 nm.

**Table 1**
The minimum inhibition concentration (μM) of imidazole-phenanthroline derivatives **1, 2 and 3** (Antibiotic; C: chloramphenicol).

| Compound/Bacteria | *B.subtilis ATCC 6633* | *P.aeruginosa ATCC 29,853* | *E.coli ATCC 35,218* | *E.faecalis ATCC 292,112* | *S.typhimurium ST-10* | *S.mutans NCTC 10,449* | *S.aureus ATCC 25,923* |
|---|---|---|---|---|---|---|---|
| **1** | 625 | 625 | 625 | 625 | 625 | 1250 | 1250 |
| **2** | 1250 | 625 | 1250 | 1250 | 1250 | 625 | 1250 |
| **3** | 156,25 | 156,25 | 156,25 | 156,25 | 156,25 | 156,25 | 156,25 |
| **C** | 9,76 | 2,44 | 312,5 | 9,76 | 78,125 | 9,76 | 156,25 |

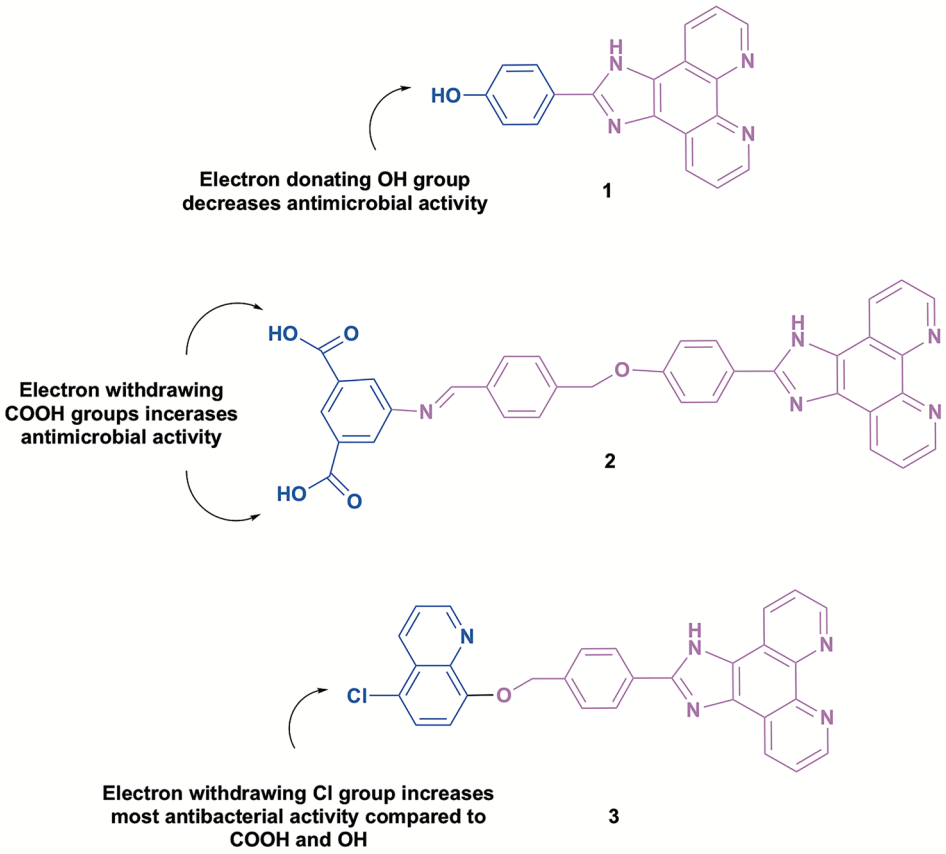


**Fig. 10.** Chemical structures and structure–activity relationships (SAR) of imidazo-phenanthroline derivatives (**1, 2** and **3**) showed potent antibacterial activities.

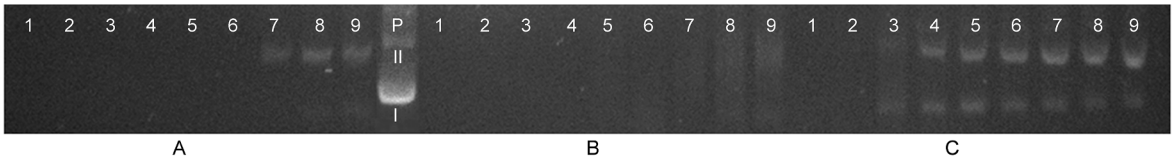


**Fig. 11.** Electrophotograms applying to the interaction of pBR322 plasmid DNA with decreasing concentrations of **2** (A), **3** (B) and **1** (C). Line P applied untreated plasmid DNA to use as a control. Lines 1–9 applied to plasmid DNA interacted with decreasing concentrations of compounds (10000 μM, 5000 μM, 2500 μM, 1250 μM, 625 μM, 321.5 μM, 156.25 μM, 78.125 μM, 39.062 μM).

## 4. Conclusion

As a summary, fluorescent imidazo-phenanthroline derivatives have been designed, prepared and characterized by various spectroscopic techniques. Their biological activities were investigated. Antibacterial activities of the compounds were determined against seven different microorganisms. The minimal inhibitory concentration (MIC) values of the compounds were studied, and these values are in the range of 156,25–1250 μM. As it is shown in Table 1, it can be seen that the most effective compound on the microorganisms was **3**. According to the results, MIC values of **3** was determined as 156,25 μM on all tested bacteria. Compared with the compounds, standard antibiotic was more effective on the bacteria. According to the DNA-cleavage study results, all imidazole-phenanthroline derivatives were found to be highly effective on DNA, even at the lowest concentrations.

## Declaration of Competing Interest

The authors declared that there is no conflict of interest.

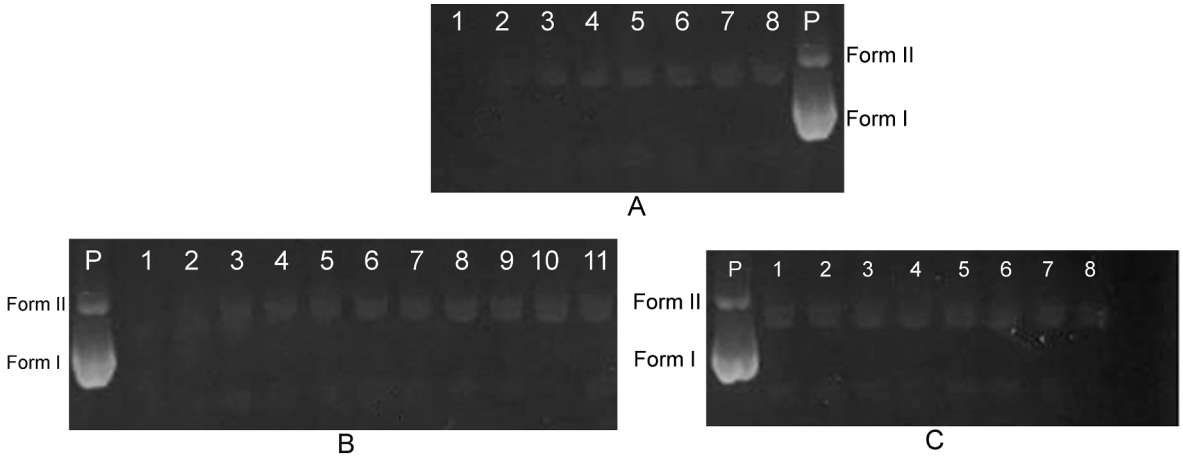


**Fig. 12.** Electrophotograms applying to the interaction of pBR322 plasmid DNA with decreasing concentrations of **2** (A), **3** (B) and **1** (C). Line P applied untreated plasmid DNA to use as a control. Lines 1–11 applied to plasmid DNA interacted with decreasing concentrations of compounds (156.25 μM, 78.125 μM, 39.062 μM, 19.531 μM, 9.765 μM, 4.882 μM, 2.441 μM, 1.220 μM, 0.61 μM, 0.305 μM, 0.152 μM).

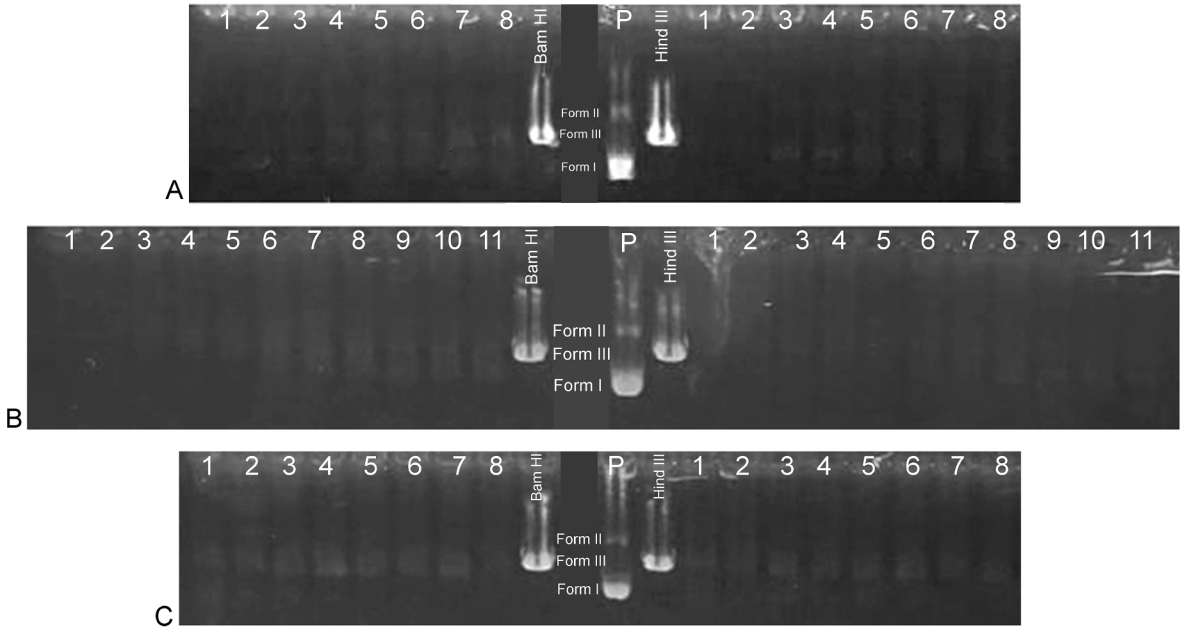


**Fig. 13.** Electrophoretogram applying to incubated mixtures of plasmid DNA and compounds **2** (A), **3** (B) and **1** (C) followed by digestion with *BamH* I or *Hind* III. Lane P: the untreated and undigested plasmid DNA. Lines *BamH* I and *Hind* III: digestions of plasmid DNA-compounds mixtures to use as a control. Lines 1–11: digestions of plasmid DNA interacted with decreasing concentrations of compounds (156.25 μM, 78.125 μM, 39.062 μM, 19.531 μM, 9.765 μM, 4.882 μM, 2.441 μM, 1.220 μM, 0.61 μM, 0.305 μM, 0.152 μM).

## Acknowledgment

We thank the Scientific Research Projects Foundation (BAP) of Selcuk University (Konya/TURKEY) for financial support of this work.

## Appendix A. Supplementary material

Supplementary data to this article can be found online at https://doi.org/10.1016/j.bioorg.2020.103885.

## References

[1] Tatiana Fonseca, Barbara Gigante, Thomas LGilchrist, A short synthesis of phenanthro[2,3-d]imidazoles from dehydroabietic acid. Application of the methodology as a convenient route to benzimidazoles, Tetrahedron 57 (9) (2001) 1793–1799.
[2] İbrahim Erden, Nebahat Demirhan, Ulvi Avcıata, Synthesis and Characterization of a New Imidazole Ligand and its Complexes with Cobalt(II), Nickel(II) and Copper (II), Synth. React. Inorg., Met.-Org., Nano-Met. Chem. 36 (2006) 559–562.
[3] Özden Tarı, Fatma Gümüş, Leyna Açık, Betül Aydın, Synthesis, characterization and DNA binding studies of platinum(II) complexes with benzimidazole derivative ligands, Bioorg. Chem. 74 (2017) 272–283.
[4] Mesut Gomleksiz, Cihan Alkan, Belgin Erdem, Synthesis, Characterization and Antibacterial Activity of Imidazole Derivatives of 1,10-Phenanthroline and their Cu (II), Co(II) and Ni(II) Complexes, S. Afr. J. Chem. 66 (2013) 107–112.
[5] Xiaowei Lei, Hongyan Wang, Yaorong Feng, Jianxun Zhang, Xuejiao Sun, Suming Lai, Zhilong Wang, Song Kang, Synthesis, evaluation and thermodynamics of a 1H-benzo-imidazole phenanthroline derivative as a novel inhibitor for mild steel against acidic corrosion, RSC Adv. 5 (2015) 99084–99094.
[6] Rosa M.F. Batista, Susana P.G. Costa, M. Belsley, M. Carlos Lodeiro, Manuela M. Raposo, Synthesis and characterization of novel (oligo)thienyl-imidazo-phenanthrolines as versatile π-conjugated systems for several optical applications, Tetrahedron 64 (39) (2008) 9230–9238.
[7] Abdoul Nzeyimana, Semra Utku, Leyla Açık, Ayten Çelebi Keskin, Synthesis, Characterization and DNA Interaction of Novel Platinum(II) Complexes Containing Substituted Benzimidazole Ligands, Rev. Roum. Chim. 62 (2017) 227–236.
[8] Rosa M.F. Batista, Susana P.G. Costa, M. Belsley, M. Manuela, M. Raposo, Synthesis and optical properties of novel, thermally stable phenanthrolines bearing an arylthienyl-imidazo conjugation pathway, Dyes Pigm. 80 (3) (2009) 329–336.
[9] Jayaraman Jayabharathi, Venugopal Thanikachalam, Marimuthu Venkatesh

Perumal, Natesan Srinivasan, Fluorescence resonance energy transfer from a bioactive imidazole derivative 2-(1-phenyl-1H-imidazo[4,5-f] [1,10]phenanthrolin-2-yl)phenol to a bioactive indoloquinolizine system, Spectrochim. Acta Part A Mol. Biomol. Spectrosc. 79 (1) (2011) 236–244.
[10] Mohan N. Patel, Promise A. Dosi, Bhupesh S. Bhatt, Antibacterial, DNA interaction and superoxide dismutase activity of drug based copper(II) coordination compounds, Polyhedron 29 (17) (2010) 3238–3245.
[11] M. Antonietta, Zoroddu, Stefania Zanetti, Rebecca Pogni, Riccardo Basosi, An electron spin resonance study and antimicrobial activity of copper(II)-phenanthroline complexes, J. Inorg. Biochem. 63 (4) (1996) 291–300.
[12] Mahboube Eslami Moghadam, Adeleh Divsalar, Abdolghafar Abolhosseini Shahrnoy, Ali Akbar Saboury, Synthesis, cytotoxicity assessment, and interaction and docking of novel palladium(II) complexes of imidazole derivatives with human serum albümin, J. Biomol. Struct. Dyn. 34 (8) (2016) 1751–1762.
[13] Shaikh Kabeer Ahmed, Shaikh Khaled, Syntheses, spectral characterization, thermal properties and DNA cleavage studies of a series of Co(II), Ni(II) and Cu(II) polypyridine complexes with some new imidazole derivatives of 1,10-phenanthroline, Arabian Journal of Chemistry, 2015 (in press).
[14] P.R. Chetana, Ramakrishna Rao, R.S. Sounik Saha, P. Policegoudra, M.S. Aradhya Vijayand, Oxidative DNA cleavage, cytotoxicity and antimicrobial studies of l-ornithine copper (II) complexes, Polyhedron 48 (1) (2012) 43–50.
[15] Hala A. El-Asmy, Ian S. Butler, Zhor S. Mouhri, Bertrand J. Jean-Claude, Mohamed S. Emmam, Sahar I. Mostafa, Zinc(II), ruthenium(II), rhodium(III), palladium(II), silver(I), platinum(II) and complexes of 2-(2′-hydroxy-5′-methylphenyl)-benzotriazole as simple or primary ligand and 2,2′-bipyridyl, 9,10-phenanthroline or triphenylphosphine as secondary ligands: Structure and anticancer activity, J. Mol. Struct. 1059 (2014) 193–201.
[16] Khalid Mahmood, Waleed Hashmi, Hammad Ismail, Bushra Mirza, Brendan Twamley, Zareen Akhter, Isabel Rozas, Robert J. Baker, Synthesis, DNA binding and antibacterial activity of metal(II) complexes of a benzimidazole Schiff base, Polyhedron 157 (2019) 326–334.
[17] Fatih Sevgi, Ugur Bagkesici, Ahmed Nuri Kursunlu, Ersin Guler, Fe (III), Co(II), Ni (II), Cu(II) and Zn(II) complexes of Schiff bases based-on glycine and phenylalanine: Synthesis, magnetic/thermal properties and antimicrobial activity, J. Mol. Struct. 1154 (2018) 256–260.
[18] Gökhan Elmacı, Halil Duyar, Burcu Aydıner, Issah Yahaya, Nurgül Seferoğlu, Ertan Şahin, Süheyla Pınar Çelik, Leyla Açık, Zeynel Seferoğlu, Novel benzildihydrazone based Schiff bases: Syntheses, characterization, thermal properties, theoretical DFT calculations and biological activity studies, J. Mol. Struct. 1184 (2019) 271–280.
[19] Divyesh C. Mungra, Manish P. Patel, Ranjan G. Patel, Microwave-assisted synthesis of some new tetrazolo[1,5-a]quinoline-based benzimidazoles catalyzed by p-TsOH and investigation of their antimicrobial activity, Med. Chem. Res. 20 (6) (2011) 782–789.
[20] Rajkumar U. Pokalwar, Rajkumar V. Hangarge, Prakash V. Maske, Murlidhar S. Shingare, Synthesis and antibacterial activities of α-hydroxyphosphonates and α-acetyloxyphosphonates derived from 2-chloroquinoline-3-carbaldehyde, ARKIVOC 11 (2006) 196–204.
[21] Yellappa Shivaraj, Malenahalli H. Naveen, Giriyapura R. Vijayakumar, Doyijode B. Aruna Kumar, Design, Synthesis and Antibacterial Activity Studies of Novel Quinoline Carboxamide Derivatives, Journal of the Korean Chemical Society, 2013, 57, 2, 241-245.
[22] Prabhpreet Singha, Subodh Kumar, Photonic logic gates based on metal ion and proton induced multiple outputs in 5-chloro-8-hydroxyquinoline based tetrapod, New J. Chem. 30 (2006) 1553–1556.
[23] Hai-Rong Zhang, Ting Meng, Yan-Cheng Liu, Zhen-Feng Chen, You-Nian Liu, Hong Liang, Synthesis, characterization and biological evaluation of a cobalt(II) complex with 5-chloro-8-hydroxyquinoline as anticancer agent, Appl. Organomet. Chem. 30 (9) (2016) 740–747.
[24] Asmaa Aboelnaga, Taghreed H. EL-Sayed, Click synthesis of new 7-chloroquinoline derivatives by using ultrasound irradiation and evaluation of their biological activity, Green Chemistry Letters and Reviews, 2018, 11, 3, 254-263.
[25] Gao-Feng Zha, et al., SAR and molecular docking studies of benzo[d]thiazolehydrazones as potential antibacterial and antifungal agents, Bioorg. Med. Chem. Lett. 27 (2017) 3148–3155.
[26] S.N.A. Lekkala Ravindar, K.P. Bukhari, H.M. Rakesh, H.K. Manukumar, N. Mallesha Vivek, Zhi-Zhong Xie, Hua-Li Qin, Aryl fluorosulfate analogues as potent antimicrobial agents: SAR, cytotoxicity and docking studies, Bioorg. Chem. 81 (2018) 107–118.
[27] K.P. Rakes, H.K. Kumar, B.J. Ullas, J. Shivakumara, D. Channe Gowd, Amino acids conjugated quinazolinone-Schiff's bases as potential antimicrobial agents: Synthesis, SAR and molecular docking studies, Bioorganic Chemistry, 2019, 90, 103093.
[28] Kadalipura P. Rakesh, Manukumar H. Marichannegowda, Shobhith Srivastava, Xing Chen, Sihui Long, Chimatahalli S. Karthik, Putswamappa Mallu, Hua-Li Qin, Combating a Master Manipulator: Staphylococcus aureus Immunomodulatory Molecules as Targets for Combinatorial Drug Discovery, ACS Comb. Sci. 20 (12) (2018) 681–693.
[29] K.P. Rakesh, H.K. Vivek, H.M. Manukumar, C.S. Shantharam, S.N.A. Bukhari, Hua-Li Qin, M.B. Sridhara, Promising bactericidal approach of dihydrazone analogues against bio-film forming Gram-negative bacteria and molecular mechanistic studies, RSC Adv. 8 (2018) 5473.
[30] Kadallipura Puttaswamy Rakesh, Suhas Ramesh, Shivakumar & Dase Channe Gowda, Effect of Low Charge and High Hydrophobicity on Antimicrobial Activity of the Quinazolinone-Peptide Conjugates, Russian Journal of Bioorganic Chemistry, 2018, 44, 158–164.
[31] Gao-Feng Zha, K.P. Shi-Meng Wang, S.N.A. Rakesh, H.M. Bukhari, H.K. Manukumar, N. Mallesha Vivek, Hua-LiQin, Discovery of novel arylethenesulfonyl fluorides as potential candidates against methicillin-resistant of Staphylococcus aureus (MRSA) for overcoming multidrug resistance of bacterial infections, Eur. J. Med. Chem. 162 (15) (2019) 364–377.
[32] Chen Li, M.B. Sridhara, K.P. Rakesh, H.K. Vivek, H.M. Manukumar, C.S. Shantharam, Hua-LiQin, Multi-targeted dihydrazones as potent biotherapeutics, Bioorganic Chemistry, 2018, 81, 389-395.
[33] Obalı, Aslıhan Yılmaz; Uçan, Halil İsmet, Preparation of Different Substitued Polypyridine Ligands, Ruthenium(II)- Bridged Complexes and Spectoscopıc Studies, Journal of Fluorescence, 2016, 26, 5, 1685-1697.
[34] Obalı, Aslıhan Yılmaz; Uçan, Halil İsmet, Ruthenium (II) Complexes of Mono-, Di- and Tripodal Polypyridine Ligands: Synthesis, Characterization, and Spectroscopic Studies, Journal of Fluorescence, 2015, 25, 3, 647-655.
[35] Katherine J. Castor, Kimberly L. Metera, Ushula M. Tefashe, Christopher J. Serpell, Janine Mauzeroll, Hanadi F. Sleiman, Cyclometalated Iridium(III) Imidazole Phenanthroline Complexes as Luminescent and Electro-chemiluminescent G-Quadruplex DNA Binders, Inorg. Chem. 54 (2015) 6958–6967.
[36] Takahiro Seki, Kunihiro Ichimura, Formation of Head-to-Tail and Side-by-Side Aggregates of Photochromic Spiropyrans in Bilayer Membrane, J. Phys. Chem. 94 (9) (1990) 3769–3775.
[37] Edwin.E. Jelley, Spectral Absorption and Fluorescence of Dyes in the Molecular State, 1936, Nature, 138, 1009–1010.
[38] Burcu Aydıner, Ergin Yalçın, Heiko Ihmels, Leyla Arslan, Leyla Açık, Zeynel Seferoğlu, Arylstyrylimidazo[1,2-a]pyridine-based donor–acceptor acidochromic fluorophores: Synthesis, photophysical, thermal and biological properties, J. Photochem. Photobiol., A 310 (2015) 113–121.
[39] Kanagarathinam Saravanan, Natesan Srinivasan, Venugopal Thanikachalam, Jayaraman Jayabharathi, Synthesis and Photophysics of Some Novel Imidazole Derivatives Used as Sensitive Fluorescent Chemisensors, Journal of Fluorescence 21 (2011) 65–80.
[40] Xu. Man, et al., Chalcone derivatives and their antibacterial activities: Current development, Bioorg. Chem. 91 (2019) 103133.
[41] Hao Liu, Sihui Long, K.P. Rakesh, Gao-Feng Zha, Structure-activity relationships (SAR) of triazine derivatives: Promising antimicrobial agents, European Journal of Medicinal Chemistry, 2020, 185, 111804.
[42] C. Bartel, A.K. Bytzek, Y.Y. Scaffidi-Domianello, G. Grabmann, M.A. Jakupec, C.G. Hartinger, M. Galanski, B.K. Keppler, Cellular accumulation and DNA interaction studies of cytotoxic trans-platinum anticancer compounds, J. Biol. Inorg. Chem. 17 (2012) 465–474.
[43] G. Eren, E. Emerce, L. Acik, B. Aydin, F. Gumus, A novel Trans-Pt(II) complex bearing 2-acetoxymethyl- benzimidazole as a non-leaving ligand (trans-[Pt(AMBi)$_2$Cl$_2$]): Synthesis, antiproliferative activity, DNA interaction and molecular docking studies compared with its cis isomer (cis-[Pt(AMBi)2Cl2]), J. Mol. Struct. 1184 (2019) 512–518.
[44] R.S. Roberts, G.A. Wilson, F.E. Young, Recognition sequence of specific endonuclease BamHI.1 form Bacillus amyloliquefaciens, Nature 265 (1977) 82–84.
[45] C. Icsel, V.T. Yilmaz, Y. Kaya, S. Durmus, M. Sarimahmut, O. Buyukgungor, E. Ulukaya, Cationic Pd(II)/Pt(II) 5,5-diethylbarbiturate complexes with bis(2-pyridylmethyl)amine and terpyridine: synthesis, structures, DNA/BSA interactions, intracellular distribution, cytotoxic activity and induction of apoptosis, J. Inorg. Biochem. 152 (2015) 38–52.